 doi:10.20944/preprints202012.0170.v1

Mini-Review

Comparing molecular mechanisms in solar NH_3 production and relations with CO_2 reduction

Domenico Mallamace[1], Georgia Papanikolaou[1], Siglinda Perathoner[1], Gabriele Centi[1,*] and Paola Lanzafame[1,*]

[1] Dept.s ChiBioFarAm and MIFT, ERIC aisbl and INSTM/CASPE, University of Messina, V.le F. Stagno D'Alcontres 31, 98166 Messina, Italy; perathoner@unime.it

* Correspondence: centi@unime.it (G.C.); planzafame@unime.it (P.L.)

Abstract: Molecular mechanisms for N_2 fixation (solar NH_3) and CO_2 conversion to C2+ products in enzymatic conversion (*Nitrogenase*), electrocatalysis, metal-complexes and plasma-catalysis are analysed and compared. It is evidenced that differently from what present in thermal and plasma-catalysis, the electrocatalysis path requires not only the direct coordination and hydrogenation of undissociated N_2 molecule, but to realize a series of features present in the *Nitrogenase* mechanism. There is the need of i) a multi-electron and -proton simultaneous transfer, not as sequential steps, ii) forming bridging metal hydride species, iii) generate intermediates stabilized by bridging multiple metal atoms, iv) have the capability of the same sites to be effective both in N_2 fixation and in COx reduction to C2+ products. Only iron oxide/hydroxide stabilized at defective sites of nanocarbons was found to have these features. This comparison of the molecular mechanisms in solar NH_3 production and relations with CO_2 reduction is proposed to be a source of inspiration to develop the next generation electrocatalysts to address the challenging transition to a future sustainable energy and chemistry beyond fossil fuels.

Keywords: molecular mechanisms; N_2 fixation; NRR; CO_2-to-C2+; CO_2RR; electrocatalysis; bioinspired

1. Introduction

N_2 fixation to directly produce ammonia by using solar energy (solar NH_3) is an emerging reaction of large interest. It is the sustainable alternative to the Haber-Bosch (HB) current industrial large-scale process of ammonia synthesis requiring the use of a fossil fuel as H_2 source and high temperatures/pressure to convert N_2 to ammonia [1-7]. HB process has been largely improved over the last century, reducing the minimum energy input from about 60 $GJ \cdot t_{NH3}^{-1}$ to the current values ranging between about 27 to 32 $GJ \cdot t_{NH3}^{-1}$ [7]. Nevertheless, ammonia production remains a main chemical process responsible for greenhouse gas (GHG) emissions, accounting for about 1.2-1.5% of the total global GHG emissions and over 350 Mtons CO_2 emissions yearly.

There are three technology generations which can be used to reduce this impact. The first generation uses CO_2 sequestration, in other words uses blue rather than grey hydrogen. The carbon sequestration adds energy cost and thus the effective CO_2 equivalent emissions reduction is lower than 30%. Being a technology already available (but adding costs and complexity), it could be used on the existing production, not likely to expand the use of ammonia. In fact, ammonia is an interesting energy and hydrogen vector, with advantages over alternative vectors in terms of amount transported by weight and avoidance of transporting back the carrier (N_2 produced is directly released to atmosphere). Advantages of NH_3 are the low cost per unit of stored energy (half year ammonia storage would cost 0.54 \$/kg-H_2 compared to 14.95 \$/kg-H_2 of pure H_2 storage [8]), higher volumetric energy density (7.1–2.9 MJ/L), easier and more widespread production, consolidated handling and distribution capacity, better commercial viability. For these reasons, ammonia was defined as a game changer [8]. However, the extension of the use of ammonia out of chemical (mainly

Preprints (www.preprints.org) | NOT PEER-REVIEWED | Posted: 7 December 2020 doi:10.20944/preprints202012.0170.v1

fertilizers) sector to become a key enabling element for future energy (low carbon) scenario would require the development of improved ways to produce ammonia directly from N_2.

Second generation HB process [1] is a multistep process, with i) production of renewable energy (RE), ii) water electrolysis to produce H_2 (green hydrogen) and then iii) use of the hydrogen in a conventional catalytic hydrogenation of N_2 (high temperature/pressure). The technology has been already demonstrated on pilot scale, by Siemens for example, and spin-off companies are already proposing it on the market, for example the SME Proton Venture in Netherlands. Inefficiencies derive from the need of multiple steps, coupling a high temperature/pressure catalytic step to an electrolyzer step operating under very different conditions and dynamics, and from the loss of energy deriving from producing H_2 molecules and their activation to react with nitrogen and generate ammonia.

H^+/e^- are the equivalent of H_2, but are the primary species generated from water oxidation in photoelectrocatalytic processes. Their direct use avoids the energy losses related to production/use of H_2 molecules. In addition, in a photoelectrocatalytic (PEC) device, all the stages from solar light adsorption to redox reactions leading to ammonia generation from N_2 and H_2O are integrated in a single device. This makes possible the development of compact artificial-leaf type devices able to produce in a distributed way ammonia as a vector to transport renewable energy or H_2, or alternatively to produce fertilizers in a decentralized way. This could be considered the third generation HB. However, an intermediate stage between the second and third generation is the development of electrocatalytic devices (driven from renewable electrical energy). This is the area of which most of the recent research on N_2 fixation (indicated often as N_2 reduction reaction, NRR) focused, together with the direct photocatalytic reduction of N_2. A selection of recent reviews on these aspects is presented in ref.s [1-7,9-20].

However, there are other ways for N_2 fixation to produce ammonia, also based on the use of RE. Renewable electrical energy could be used to generate a non-thermal plasma (NTP), which is a (partially) ionized gas, consisting of neutral species (molecules, radicals, excited species), ions, photons, and electrons [21]. In an NTP, the electron temperature is largely higher than the temperature of the other species and thus the radicals and excited species are formed close to ambient temperature. In combination with a catalyst (plasma-catalysis [22,23]), NTP is a valuable alternative to conventional catalysis, because generates directly activated species under ambient conditions. The control of the selective path of transformation deriving from the presence of a catalyst, allows to explore new paths to produce chemicals by using renewable energy sources. Plasma catalytic ammonia synthesis represents thus an alternative to photo- and/or electro-catalytic routes [24,25].

On the other hand, enzymatic conversion of N_2 to NH_3 on *Nitrogenase* is the reference for a sustainable N_2 fixation using indirectly solar energy. However, from a practical perspective, being required energy consumption in the form of ATP (adenosine triphosphate) and to synthesize the reducing agents and proton sources, the overall energy for nitrogen fixation is higher than for the HB process [26]. Nevertheless, in terms of reaction mechanism [27] it remains a valuable reference to understand better the possibilities for N_2 fixation at ambient conditions, as occurs in photo- and/or electro-catalytic processes as well as in plasma-catalysis.

A comparison between the different molecular mechanisms of N_2 fixation could offer a better understanding of analogies and differences, and thus provide an inspiration to design better systems. In fact, notwithstanding the many reviews of N_2 fixation, a better comparison between the mechanisms of these different approaches would be useful.

There is, in addition, a further interesting aspect and motivation for this comparison. *Nitrogenase* can reduce CO_x to hydrocarbons forming compounds such as ethylene, ethane, propylene, and propane [28-30]. This is also somewhat unique for this enzymatic system. The photo-/electro-catalytic reduction of CO_2 (CO_2RR) to form >C1 products is an attractive reaction for the possibility to build a new value chain in the conversion of CO_2 and form high-added value chemicals and fuels [31]. Producing directly C2-C3 olefins or oxygenated compounds from CO_2 would provide a direct path to overcome the use of fossil fuels [32]. There is a large debate in literature on the molecular mechanisms of C-C formation in CO_2 photo-/electro-catalytic conversion and quite discordant

Preprints (www.preprints.org) | NOT PEER-REVIEWED | Posted: 7 December 2020 doi:10.20944/preprints202012.0170.v1

hypotheses [33-38]. In NRR there are also quite dissimilar proposed reaction mechanisms and nature of the active sites, despite the relatively limited variations in the performances [39].

An analysis and comparison of the molecular mechanisms of solar NH_3 production and CO_2 reduction to >C1 products, particularly on systems able to give both reactions, by using *Nitrogenase* as reference of a molecular system able to perform both reactions, could thus provide clues for a better interpretation of the mechanistic aspects of these challenging reactions.

2. Mechanisms in *Nitrogenase*

Nitrogenase is a unique system able to convert N_2 to NH_3 [27]. Total cost of N_2 reduction corresponds to eight electrons transferred and 16 MgATPs hydrolysed. There are three classes of *Nitrogenase* differing for the heterometal atom present in the active site metal cluster (Mo, V or Fe), but the Mo-dependent nitrogenase is the most important and best studied enzyme [40]. It contains two metallo-components, *dinitrogenase* [molybdenum–iron (MoFe) protein] and *dinitrogenase reductase* (Fe protein), which associate and dissociate in a catalytic cycle also requiring a reducing source and MgATP [41]. The MoFe protein contains two metal clusters: the iron–molybdenum cofactor (FeMo-co) [42], which provides the active site for substrate binding and reduction, and P-cluster, involved in electron transfer from the Fe protein to FeMo-co [43]. The FeMo-cofactor is thus the key element for the mechanism of N_2 fixation. It contains also interstitial carbon [44] which is a key for the CO_2 conversion mechanism providing stability to the complex. Figure 1a reports the model of FeMo-cofactor, while Figure 1b the proposed mechanism of N_2 fixation [27].

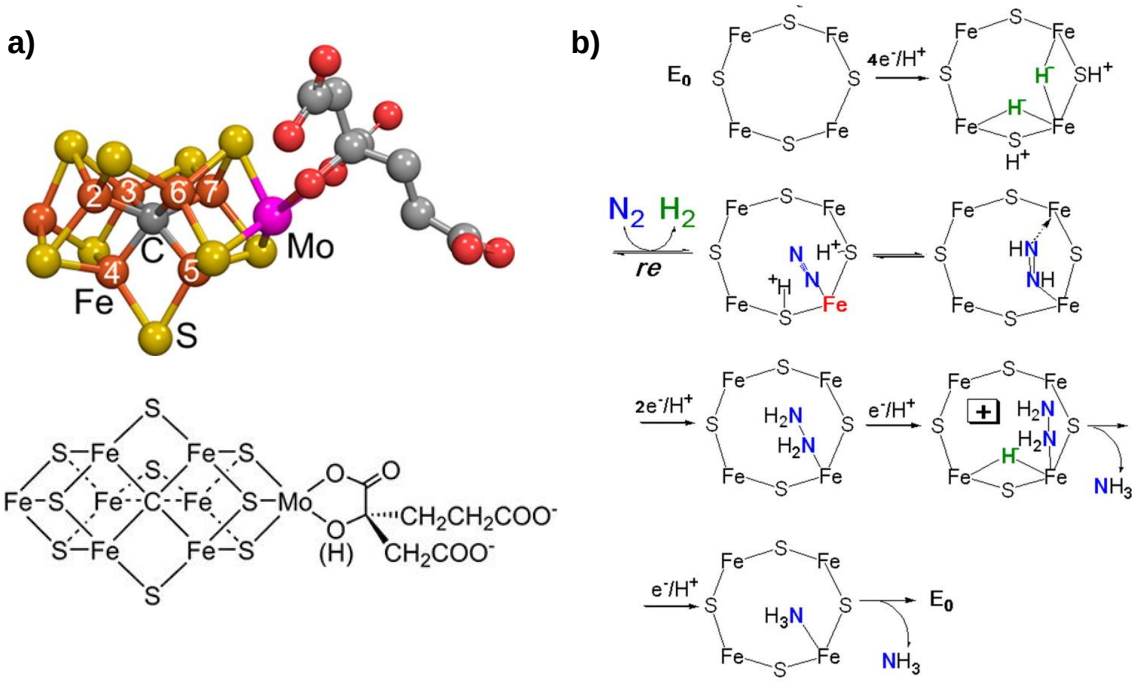

Figure 1. (a) FeMo-cofactor (Fe in rust, Mo in magenta, S in yellow, C in gray, and O in red); (b) Mechanism (key elements) of N_2 fixation on FeMo-Co. Adapted from ref. [27]. Copyright 2014 American Chemical Society.

The key features of this mechanism [45,46] are the following:

i) the presence of a specific binding site for N_2 able to first accept four electrons/protons to form two [Fe–H–Fe] bridging hydrides,
ii) coordination of N_2 on an iron sites with simultaneous reductive elimination of H_2,
iii) multi-electron/proton transfer to coordinated undissociated N_2 molecule to form a N_2H_2 molecule stabilized by interaction with two iron atoms,
iv) further multi H^+/e- transfer to form an end-on N_2H_4 coordinated molecule,

Preprints (www.preprints.org) | NOT PEER-REVIEWED | Posted: 7 December 2020 doi:10.20944/preprints202012.0170.v1

v) further steps of H^+/e^- transfer with stepwise release of ammonia.

The simultaneous electron/proton transfer to undissociated coordinated N_2 molecule is a different feature with respect to the mechanisms occurring in iron catalysts for high temperature/pressure HB process, where the first (rate limiting) step is the dinitrogen dissociative chemisorption followed by sequential hydrogenation of the intermediates [47-50]. The reason of the difference in the mechanism is that the nitrogen molecule dissociation path, in principle, is preferable being possible a sequential series of steps of electron transfer and hydrogenation of the nitrogen adatoms. However, the strongly bound nitrogen species formed by dissociation require high temperatures to avoid the catalyst inhibitions, and therefore the need of high pressure of operations (being an exothermic reversible reaction). For the N_2 molecule undissociated activation, a sequential series of electron and proton transfer steps would generate high-energy intermediates [51]. For example, the addition of one electron and one proton to N_2 to form a N_2H^* species requires −3.2 V vs. NHE (normal hydrogen electrode). For multi-electron reduction processes, for example to produce $N_2H_5^+$ adspecies, the reduction potential becomes -0.23 V. Multielectron reactions are thus necessary in the low-temperature profile, in agreement with what observed for *Nitrogenase* and to avoid/minimize the side reaction of H^+/e^- recombination to form H_2, which is possible also in the enzyme path.

As a slight change, more recent indications on the mechanism [52] suggest instead the formation of a Janus intermediate, i.e. the formation of a symmetric hydride structure with a following diazene intermediate (Figure 2).

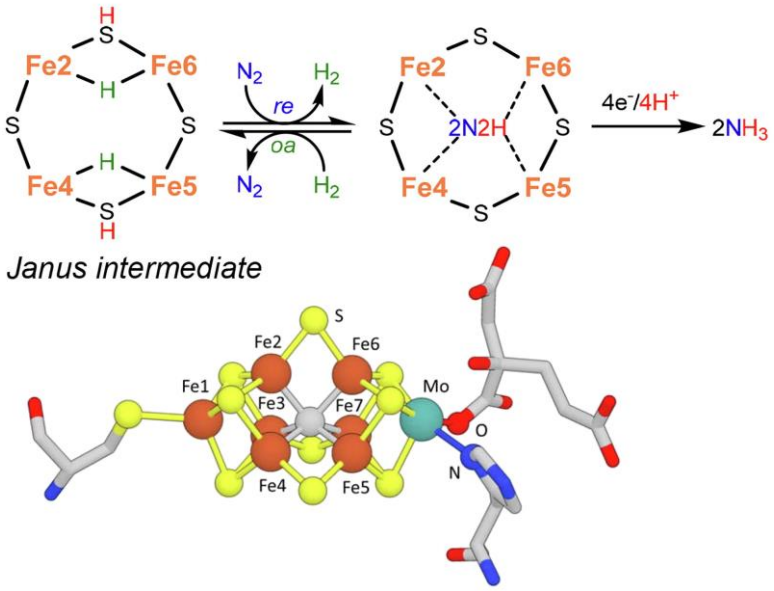

Figure 2. Key step for biological N_2 fixation and structure of nitrogenase FeMo-co. Adapted from ref. [52]. Copyright 2021 Elsevier.

Nitrogenase, although particularly in the vanadium form [53], is also able to catalyse the reductive carbon–carbon coupling of COx into hydrocarbon products, as indicated before. This is also an unique feature and suggest a role of this enzyme as an evolutionary link between the nitrogen and carbon cycles on Earth [28]. The mechanism of C-C coupling is not fully clear, but progresses have been made recently [54]. From CO_2, the mechanism involves a first step of reduction of CO_2 to CO by the Fe protein ($[Fe_4S_4]^0$) of *Nitrogenase* catalyses [55], followed by the reductive carbon–carbon coupling of two coordinated CO molecule on the same active site of *Nitrogenese* cofactor proposed for N_2 fixation (M-cluster). The tentative mechanism is presented in Figure 3.

The same type of Janus intermediate proposed for N_2 fixation (symmetric hydrides structure) reacts with two CO molecules (produced on the Fe protein) to form an ethyne like intermediate which can be hydrogenated to ethylene or could react further to form a ferracycle (formed by C_2H_4 binding

Preprints (www.preprints.org) | NOT PEER-REVIEWED | Posted: 7 December 2020 doi:10.20944/preprints202012.0170.v1

to one of Fe atoms [56]) leaving other Fe free to form other Fe-hydrides species and further coordinate CO, which can react with the ferracycle species, to give C2 products (hydrocarbon, oxygenated chemicals) (Figure 4).

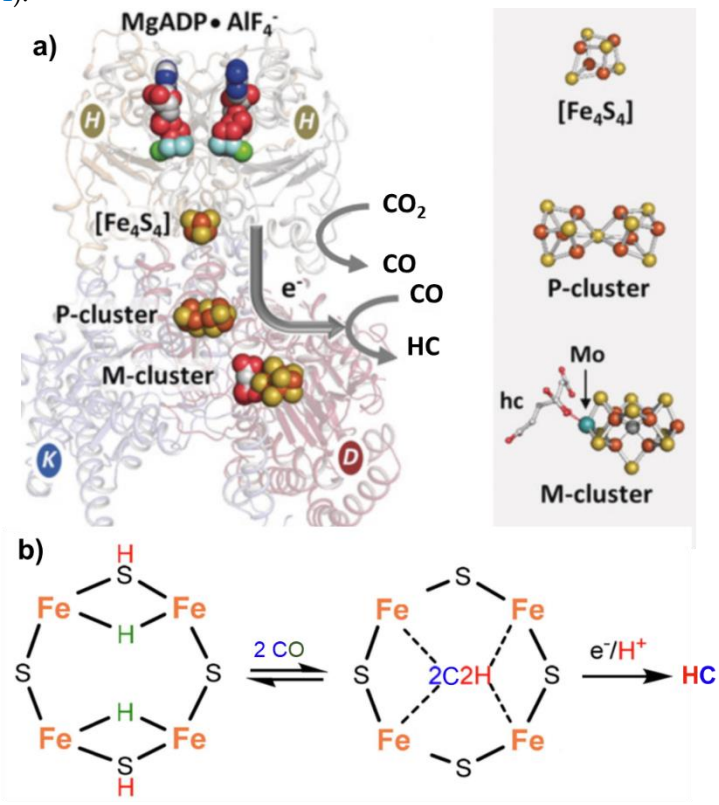

Figure 3. (**a**) Nitrogenase enzyme with indications of the key components involved in electron transfer, including MgADP·AlF_4–, [Fe_4S_4] cluster, P-cluster, and M-cluster with indication of the active centers involved in CO_2 to CO and CO_2 to hydrocarbons (HC) conversion. Adapted from ref. [28]. Copyright 2016 Wiley. (**b**) Proposed schematic mechanism of the active sites in FeMo co-factor (M-cluster) for conversion of CO to HC.

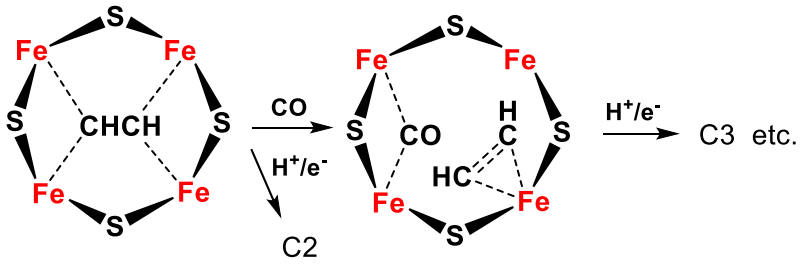

Figure 4. Proposed schematic mechanism of the active sites in FeMo co-factor for conversion of C2 intermediate to C3 products (hydrocarbon, oxygenates) via formation of a ferracycle species.

3. Bioinspired approaches

Several bioinspired approaches have been developed to mimic the nature of the active centres present in *Nitrogenase* [52,57]. As commented above, the active site (E_o in Figure 1b) able to host the dinitrogen binding after initial formation of the dihydride species (the Janus intermediate shown in Figure 2) possess vacant coordination sites [54]. Bioinspired mechanistic studies have thus focused on producing the presence of coordinatively unsaturated iron centers for N_2 binding and the formation of hydrides. However, the key mechanistic issue evidenced before, e.g. the presence of a simultaneous multi-electron/proton transfer, has been not typically considered. Four electrons and four protons must be accumulated on the FeMo-co resting state to generate the Janus intermediate (Figure 2) responsible for N_2 binding and conversion. The Janus intermediate contains two [Fe-H-Fe]

Preprints (www.preprints.org) | NOT PEER-REVIEWED | Posted: 7 December 2020 doi:10.20944/preprints202012.0170.v1

units and two protons located on bridging sulphides [58]. Four coordinatively unsaturated iron sites cooperate for accumulating electrons /protons as bridging hydrides, whilst avoiding changes in the formal oxidation state of the metal core. Dihydrogen release in a reductive elimination pathway makes available the two remaining reducing equivalents for N_2 coordination and the first stage of its reduction to form a diazenidometal complex.

Note, however, that there are still open questions regarding the N_2 fixation mechanism, such as (i) the sequence of proton/electron transfers on the N_2 unit, (ii) when ammonia release occurs (distal and alternating mechanistic pathways [59]), and (iii) if and how the molybdenum center [60] and the central carbide [61] influence the reactivity of the FeMo-co for N_2 binding and reduction. This in addition to a likely role of the central carbide in stabilizing the complex and coordinate the diazene or ethyne intermediate. However, these could be considered secondary aspects in terms of developing molecular complexes analogous to *Nitrogenase* active centers.

The bioinspired metal-complexes reported in literature focused on the coordination of N_2 molecule and the presence of sites (especially metal hydride) able to hydrogenate the coordinated nitrogen molecule. Several molecular coordination complexes show activity in N_2 binding and reduction [62-64]. Starting from the first example of systems for N_2 fixation and reduction, based on single molybdenum [65] or iron [66] centers, many other metal complexes have been also developed [62], including the use of different metal centres such as V, Co, Ru, Os, W, and Ti. Note that mechanistic studies refer typically to discrete e^- and H^+ transfer steps, although concerted proton-coupled electron transfer (PCET) steps have been not excluded (even if their occurrence not typically demonstrated). These mononuclear metal complexes were not active for multi-electron/proton transfer. The studies were focused on the synthesis and mechanistic aspects, rather than on the performances. Several of these metal complexes show some activity in the conversion of N_2 to NH_3, although typically under conditions of difficult practical utilization. Moreover, the rates of reactions and efficiencies were low. Few of them, and mainly supported phtahlocyanines were tested under electrocatalytic conditions, but not showing relevant performances [62]. Thus, while these studies provided good mechanistic insights, the advances in terms of development of effective catalytic systems for N_2 to NH_3 conversion were limited. These studies on mononuclear metal complexes does not reproduce the main key features of *Nitrogenase* being not present multi-metal centers and therefore a multi-electron/proton mechanism, although the sequence of hydrogenation of undissociated N_2 is typically present. End-on coordination of N_2 is the most considered situation, but two mononuclear complexes can operate in synergy (pairing) to coordinate in a bridging mode the N_2 molecule.

Activation of dinitrogen by polynuclear metal complexes was reviewed recently by Singht et al. [63]. To circumvent the low reactivity of N_2 (high reductive potential for one electron reduction, low proton affinity and high ionization potential of dinitrogen), and weak interaction with transition metal ions (lack of a dipole moment and relatively high energy π^* orbitals result in N_2 being a poor σ-donor and π-acceptor), the mononuclear systems strategy is based on the use of reducing metal centers (i.e., formal Fe^0 centers), while in multinuclear systems it is possible to coordinate N_2 in a bridge mode to weaken the N≡N bond and thus make nitrogen susceptible to protonation.

Different modalities of dinitrogen-derived bridging ligand(s) coordinated to multiple redox-active centers has been validated experimentally [63] and summarized in Figure 5a. Figure 5b instead reports the possibilities to weaken the N≡N bond forming diazenido-, hydrazido-, or nitrido-metal species. This is thus an alternative to activate N_2 molecule with respect to a proton-coupled electron transfer (PCET) mechanism.

There are different examples of N_2 activation by multi-metallic complexes [63]. Mostly, however, they are stoichiometric complexes and not involved in a catalytic cycle. How to translate this wide body of knowledge on the cooperative N_2 activation in multi-metallic systems to develop effective catalysts for N_2 fixation (besides the often-existing problem of cost and stability of the proposed complexes) is still a challenge. In comparison with the *Nitrogenase* mechanism, it may be commented that the formation of multi-metal-bound intermediates is part of the mechanism, which occurs

Preprints (www.preprints.org) | NOT PEER-REVIEWED | Posted: 7 December 2020 doi:10.20944/preprints202012.0170.v1

typically at the same time of hydrogen transfer to the coordinated N_2, differently from what studies in these multi-metallic complexes show.

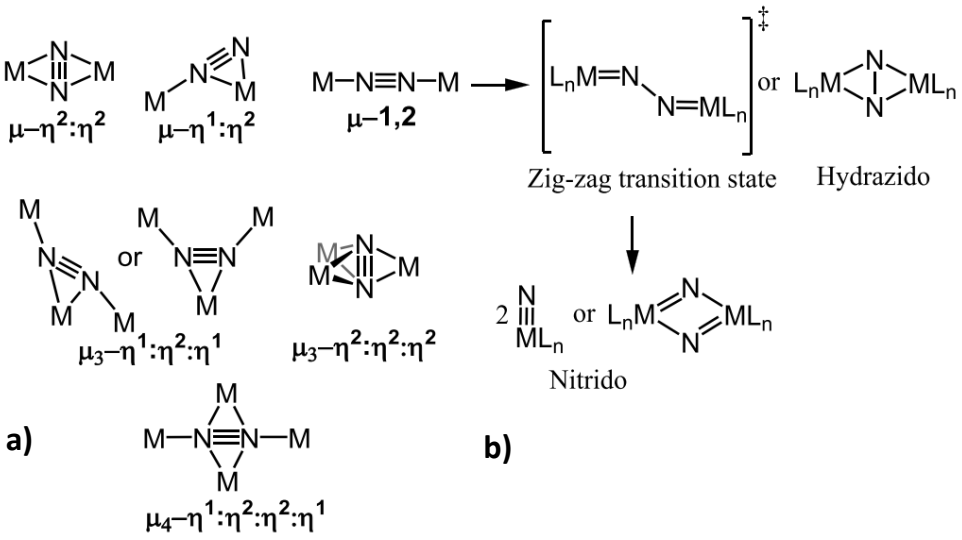

Figure 5. (**a**) Binding bridging modes of N_2 in polynuclear metal complexes. (**b**) Proposed dimetallic N_2 scission mechanism. Adapted from ref. [63]. Copyright 2020 American Chemical Society.

Transition metal–sulphur (M-S) compounds are a third class of inorganic systems investigated for N_2 activation, and they clearly can be considered directly bioinspired starting from the active centers present in *Nitrogenase*. Three classes of M–S compounds were reviewed by Tanifuji and Ohki [64]: (i) multinuclear M–S clusters structurally or functionally relevant to the *Nitrogenase* cofactors, (ii) mono- and dinuclear transition metal complexes supported by sulphur-containing ligands in N_2 and N_2H_x (x = 2, 4) chemistry (thus mimicking intermediates in the mechanism of N_2 fixation), and (iii) metal sulphide-based solid materials employed in the reduction of N_2. However, only for the latter class, reactivity data have been reported, while there are less information on the molecular mechanisms and thus in providing insights on how to translate toward solid materials the mechanistic indications provided by the *Nitrogenase* enzyme. Thus, the Tanifuji and Ohki [64] indications were that "with regard to the reactivity studies of M–S clusters, catalytic N_2 conversion still remains a challenge, while substoichiometric N_2 reduction has been recently achieved."

In conclusion, this short analysis of the studies on N_2 activation and bioinspired approaches in metal complexes indicates that notwithstanding the large synthetic and characterization effort, the indications on how to design robust and active solids which can reproduce enzymatic mechanisms of N_2 to NH_3 conversion remain elusive.

4. From electrocatalysis to biomimicking mechanisms

The previous section showed how the current state-of-the-art approaches in biomimicking metal complexes, although being active in N_2 coordination and in part in the further conversion to NH_3, do not well describe the key features in the proposed mechanism for *Nitrogenase*, neither its ability for both N_2 fixation as well as to give products with C-C bond formation (indicated as C2+ products, hereinafter) in CO_x conversion. In addition, the realization of a full catalytic cycle for N_2 to NH_3 conversion with high turnover number (TON) is still a challenge. It is thus worth to look whether, among the existing electrocatalysts, there are systems active in both N_2 fixation (NRR) and formation of >C1 products in CO_2 conversion (CO_2RR), and which have features which may resemble those for the active sites for *Nitrogenase*.

A relevant example is given by electrocatalysts based on iron-oxide on carbon nanotubes (CNT, multiwalled). These electrocatalysts were among the first identified to be active in the formation of >C1 products (hydrocarbon, oxygenated chemicals) in CO_2 electrocatalytic conversion, particularly

Preprints (www.preprints.org) | NOT PEER-REVIEWED | Posted: 7 December 2020 doi:10.20944/preprints202012.0170.v1

in isopropanol synthesis, an extremely challenging reaction being a 18e⁻ reduction [67,68]. Note that earlier studies and still several theoretical studies instead indicated that only over particular copper faces (the [100] face) the formation of C2 products in the electrochemical conversion of CO_2 is possible [69,70]. On these copper systems, the involvement of coupling reactions between surface adspecies is suggested as the path to produce multi-carbon products, by dimerization of two chemisorbed CO molecules on metallic copper [71,72], a chemisorbed CO and other intermediates such as CHO [73] or the reaction of chemisorbed CO with adsorbed acetaldehyde (H_3C-C=O) to form C3 products (1-propanol) [74]. Chan et al. [75] suggested that Cu(100) planes with surface strain induced by compression and elongation of perpendicular axes is geometrically beneficial for C2 product formation; by stabilizing the CO in bridge sites they infer a low activation energy for CO–CO coupling. Note that all these mechanistic indications refer to metal surfaces, and not to oxide nanoparticles, while there are several indications that the oxide or derived one (such as hydroxide) are the active species. In addition, none of these systems reported as active in CO_2 electrochemical conversion to >C1 hydrocarbons or oxygenated compounds, is active also in N_2 fixation, differently from the iron oxide on CNT electrocatalyst [76,77].

Recent results [78] have demonstrated that the active phase in these systems for N_2 fixation is a metal oxide, at least in the ex-situ situation, because operando NEXAFS (near edge X-ray absorption fine structure) results combined with ambient pressure XPS data show the in-situ formation of a FeOOH species stabilized at carbon defect sites during the electrocatalytic reaction [79].

During N_2 fixation, the Fe_2O_3/CNT electrocatalyst transforms in-situ, and if after 3h of operation, the electrocatalyst is removed and washed, most of the iron-oxide (weakly interacting with the carbon support) could be leave only very small (≤ 2 nm) iron-oxide nanoparticles, sitting at defects of CNTs [80]. Their characterization show that they have been transformed in-situ to a maghemite (γ-Fe_2O_3) structure with respect to the initial hematite (α-Fe_2O_3) structure. This transformation leads to an about five times increase of both ammonia formation rate and Faradaic selectivity to ammonia, likely due to the in-situ formation of a γ-FeOOH rather than α-FeOOH nanostructure (as for hematite).

Figure 6a reports the proposed optimized FeOOH/N-C interface nanostructure (where N-C indicates the N-doped nanocarbon) which forms by application of a negative potential within the range of relevance for the electrocatalytic behaviour. The relevance of the specific nanostructure derives from the observation, as remarked in Figure 6b, of strong analogies between the surface arrangement in γ-FeOOH [31] and the suggested mechanism of reductive conversion of N_2 in the *Nitrogenase* FeMo-cofactor discussed above. Although S atoms are not present, the surface structure of γ-FeOOH present biomimetic sites able to give a concerted multi/electron and /proton reductive transfer mechanism and N_2 or CO coordination as those reported in Figure 2 (N_2 fixation) and Figs. 3-4 (CO_2 reduction to multi-carbon species).

Note that this type of sites, different from other hypotheses on molecular mechanisms for both NRR and CO_2RR (to >C1 products), could well explain why these electrocatalysts are active in both reactions as *Nitrogenase*. The application of the mechanism proposed for C3 products in *Nitrogenase* (Figure 4) could also well explain why experimentally the formation of isopropanol is observed, while theoretical approaches predict the formation of the linear C3 alcohol (1-propanol) [74]. Furthermore, the model of the nature of the active sites outlined in Figure 6b, is well in agreement with the experimental observation that the oxide is the active species in the electrocatalytic reaction rather than the metal or a nitride species [78].

Although the model proposed in Figure 6b is not proven, except in terms of in-situ formation of a FeOOH species during the electrocatalytic reaction [79], the point remarked above well support this hypothesis and stimulate the need to explore more in depth this possibility of biomimicking electrocatalysis. There is the need to prove and identify better the nature of these surface sites, and especially investigate how to enhance their formation, to increase the performances, which, however, are already among the best reported values for both N_2 fixation and CO_2RR to >C1 products. There is an undoubted role of carbon defects for the stabilization of this type of species, and the high-resolution transmission electron image (HRTEM) presented in Figure 6a well evidence that the iron-oxide/hydroxide nanoparticles are sitting at carbon defects.

Preprints (www.preprints.org) | NOT PEER-REVIEWED | Posted: 7 December 2020 doi:10.20944/preprints202012.0170.v1

Thus, although different reaction mechanisms could be also possible for both NRR and CO_2RR, the mechanism suggested based on biomimetic sites of those present in *Nitrogenase* and able to i) give multi/electron and /proton transfer, ii) chemisorb N_2 and vicinal CO molecules (bridging multiple Fe atoms) and iii) generate as well nearlying hydride species also bridging Fe atoms, is quite attractive for the possibility to explain many experimental features, at least on these electrocatalysts.

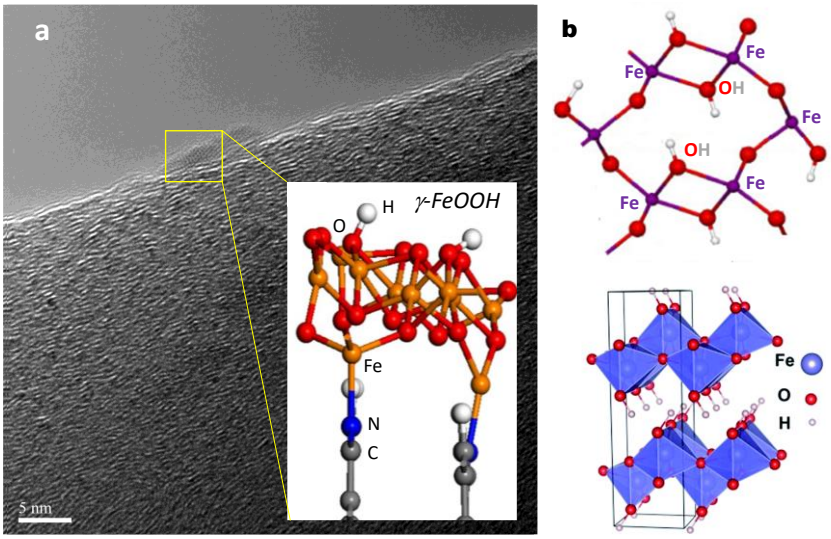

Figure 6. (**a**) HRTEM of activated iron-oxide/CNT electrocatalysts for NRR (adapted from ref. [80]. Copyright 2020 Elsevier), with the inset reporting a lateral view of the optimized ferrihydrite nanostructures decorating the N-doped graphitic zigzag edges (adapted from ref. [79]. Copyright 2018 Springer Nature). (**b**) Proposed γ-FeOOH (bottom) nanostructure and related surface structure (top) for simultaneous multi/electron and /proton transfer in NRR and CO2RR (for the last to >C1 products). Adapted from ref. [31]. Copyright 2019 Elsevier.

5. Other proposed molecular mechanisms of reaction

A large variety of reaction mechanisms and associated nature of the active sites have been proposed in literature. To focus discussion, we limit here analysis to suggested hypotheses, typically based on an DFT theoretical approach, for nanocarbon-based electrocatalysts for NRR [39]. This analysis is also representative of the general state-of-the-art of the sector. Note that results reported in literature for N_2 fixation at ambient temperature and pressure, using H_2O as the hydrogen source range typically between 0 and 20% as Faradaic selectivity and specific current density (mA/cm^2) between 0.05 and 0.2. Although there are variations, industrial targets should be a Faradaic selectivity higher than 80% and specific current density higher than 20-50 mA/cm^2 [39]. From this perspective in terms of industrial targets, all reported results result quite similar and hardly justify a very large of proposed reaction mechanisms with different nature of the active sites.

In fact, a non-exhaustive list of the proposed nature of the active centers in N_2 fixation is the following:

1. presence of C=O and O-C=O groups in graphene sheets [81]
2. electron-deficient environment at the B-doping positions in Boron-doped graphene [82]
3. P atoms substituting C atoms in phosphorus-doped carbon nanotubes [83]
4. pyridinic and pyrrolic N in N-doped porous carbons [84]
5. defective nature of carbon-doped boron nitride nanosheets [85]
6. sp^2-hybridized B, due to substitution of an edge N atom in the cavity of C_2N [86]
7. double boron atom species in defect cavities of C_2N [87]
8. atomically dispersed Ni sites in a carbon matrix [88]
9. heteronuclear dual-atom catalytic elements in FeMo/g-C3N4 [89]

Preprints (www.preprints.org) | NOT PEER-REVIEWED | Posted: 7 December 2020 doi:10.20944/preprints202012.0170.v1

10. iron atoms in iron-phthalocyanine (FePc) grafted on O-MWCNT (oxygen-functionalized multiwalled carbon nanotubes) [90]
11. oxygen vacancies in $NiCo_2O_4$ on hollow N-carbon polyhedra [91]
12. copper atoms on activated carbon functionalized with sulfonated groups [92]

It is evident from the above indications that a very large variety of hypothesis on the nature of the active sites in NRR have been proposed (this limited to only nanocarbon-based electrodes), even though performances were in a relatively narrow range and quite far from the industrial need, as commented above. The nature of the active sites is going from sites related to modifications of the nanocarbon itself (defect sites, carbon atoms with charge density due to strains and/or defects, different type of heteroatoms, isolated metal ions or metal dimers inserted in carbon defects) or to supported metal atoms or nanoparticles.

From the perspective of biomimetic systems of *Nitrogenase*, none of the above electrocatalysts can be considered to have the key features of the active sites in the enzyme, and even if not specifically investigated, the systems were not among those reported able to convert CO_2 electrocatalytically to >C1 products (multi-carbon) and thus able to perform reaction of carbon-carbon coupling during electrocatalysis.

The iron-oxide/nanocarbon system discussed in the previous section thus remains an unique system in terms of capability of good performances in both NRR and CO_2RR (to >C1 products) as *Nitrogenase*, with sites that can mimic those in *Nitrogenase*, even if their catalytic role was only indirectly proven.

In multi-carbon CO_2RR a quite large range of mechanistic hypotheses has been also indicated sometimes on the bases of theoretical modelling [72-75,93-102]. The proposals are different in terms of the mechanism, type of intermediates and of active sites. For example, Han et al. [102] indicate Cu catalytic sites sitting at defects of N-doped porous carbon materials as effective. The pyridinic N species react with CO_2 to produce CO and together with Cu catalytic sites act cooperatively to produce C_2H_5OH and C_3H_7OH via a two-site mechanism. Marepally et al. [101] analysing the behaviour of Cu and Fe based dendritic-type electrodes reported that the nano-morphology influences positively not only the activity, but especially the selectivity to >C1 products (i.e. ethanol, isopropanol, acetic acid) when smoother edges and denser surface sites are present. Genovese et al. [100] indicate a mechanism of >C1 formation (acetate) involving the reaction between CH_x adspecies (formed by reduction of CO_x) on copper nanoparticles and the carbon dioxide anion radical (formed by one electron transfer to CO_2) present in the double layer. Lum et al. [99] indicated that high selectivity to C2+ products is attained at overpotential conditions (−1 V vs RHE) where the current density is sufficiently high to induce (due to mass diffusion limitations) an increase of the pH near the catalyst surface. It is thus not a role of specific active sites, but of controlling the local conditions (three-phase boundary, pH, etc.) at the electrocatalyst/electrolyte interface. Sen et al. [98] indicated that surface confinement (in copper nanofoams), and thus again change of the local situation at the electrocatalyst-electrolyte interface, the key for C2+ products. Zhang et al. [97] also indicated that Cu_2O nanocavities (are necessary for CO_2 reduction to ethanol through the confinement of the CO intermediate. Zhuang et al. [96] also indicate Cu_2O nanocavities as necessary to confine the intermediates and allow the formation of C2+ products.

This group of authors thus emphasise the confinement of intermediates near the surface as the key aspect to form multi-carbon products. Other authors instead indicate the need to have specific surface sites on the electrocatalyst. Li et al. [95] indicated that CO_2-to-C2+ conversion requires an enriched disorder in the copper compared to crystalline Cu, obtained by electrochemical nanocrystal scrambling, i.e. the dynamic fusion of Cu nanoparticles under CO_2 reducing conditions to form multi-carbon-active scrambled nanocrystals. It is not well described which new type of active sites forms in this scrambling mechanism, and the influence on the mechanism, but it is hypothesized that lead to a higher population of strongly bound *CO, due to disorder-induced microstrain that alleviate the undesired repulsive interactions of a high density of bound *CO [103], comparable to the creation of optimal geometries in enzymatic systems.

Preprints (www.preprints.org) | NOT PEER-REVIEWED | Posted: 7 December 2020 doi:10.20944/preprints202012.0170.v1

These mechanisms indicate the need to have a metallic Cu surface to form C2+ products, and analogously Munir et al. [94] indicated that C–C coupling is favoured on Cu^0 sites rather than Cu_2O. Chan et al. [75] modelling copper(100) faces with surface strain found that surface strain with one compressed axis and one elongated axis is geometrically beneficial for C2 product formation. The surface strain stabilizes the CO binding on the bridge sites ($*CO_{bridge}$) and the C2 intermediates –*OCCOH and *OCCO which maintains a low activation energy of CO–CO coupling. The surface strain also suppresses *H formation. These sites are also active in C3 formation. Goodpaster et al. [73] indicated that Cu(100) is necessary for the mechanism of C–C bond formation occurring through a CO dimer at low potential (formed at adjacent Cu sites), while at high potential C–C bond formation occurs through reaction of adsorbed CHO and CO forming an $OCCHO_{ads}$ species (intermediate also in the CO dimer path) further hydrogenated to ethylene.

A group of other authors instead indicate that oxide or hydroxide species are those active in CO_2 electrocatalytic conversion. Eilert et al. [93] indicated Cu_2O nanocubes or copper(II)–carbonate/hydroxide are the active species in multi-carbon bond formation. Chang et al. [74] indicate Cu_2O derived Cu as the active element, with the C–C coupling mechanism between CO and surface-bound acetaldehyde as the key step to form C3 (1-propanol), while hydrogenation of the acetaldehyde gives the C2 alcohol (ethanol). The surface-bound acetaldehyde is indicated as the intermediate reported in literature [104], even though this indication is questionable. Results indicate an enol-like surface intermediates (on metallic Cu surface) involved in the formation of multi-carbon products.

Even if this short survey is not exhaustive of the many different indications of the surface mechanisms in the electrocatalytic conversion of CO_2 to C2+ (multi-carbon) products, it is evident that there are quite discordances on the nature of the active sites, and even on the surface oxidation state. Most of the papers claims an unique behaviour for copper electrocatalysts, but as mentioned above, iron-based catalysts (oxide/hydroxide) behaves even better in forming C2+ products [67,68,105,106] and even Pt, a metal typically considered unable to give C2+ in the electrocatalytic conversion of CO_2, may reach selectivity to C2+ > 60% under specific conditions of reaction [107,108]. The proposed mechanism and nature of the active sites are typically unable to explain a single type of mechanism/active sites able to explain the behaviour both in N_2 fixation (NRR) and CO_2 reduction to multi-carbon products, as present in *Nitrogenase* and the supported iron catalysts described in the previous section.

Although different types of mechanisms and nature of the active sites could exist, we believe that the search of systems active in both reactions which mimic *Nitrogenase* is a valuable direction to develop these electrocatalysts and make the necessary breakthrough advance in the field.

6. Molecular mechanisms in plasma-catalysis

As introduction to this section, it should be clarified that there are two broad categories of plasma, thermal and non-thermal. Thermal (equilibrium) plasma is a partially ionised gas with the temperature of the charged particles close to that of the neutral particles, with thus temperatures of the order of 1000-3000 K. Non-thermal (non-equilibrium) plasma (NTP) is instead characterized by the smaller charged species (electrons) having a temperature several orders of magnitude higher than that of neutral molecules. Using NTP approach, it is possible to generate high-energy species which can activate molecules while keeping the reaction temperature and energy consumption low. In this way, excited dinitrogen species (N_2*) obtained by collisions with highly energetic electrons can be obtained, for example via this reaction:

$$e^- + N_2 \rightarrow e^- + N_2* \quad (1)$$

Once formed, excessive energy stored in vibrational modes may be efficiently provided for chemical reactions. This is typically a gas-phase chemistry. H_2O should be used rather than H_2 to make the process more sustainable and reduce costs. However, yields of ammonia and energy efficiencies are still unsatisfactory [21,24,109], although they strongly depend on the type of plasma reactor configuration and mode of operation (pulsed plasma, for example). In terms of process design, it could be preferable to form NOx from N_2 in a NTP reactor and then make the catalytic

Preprints (www.preprints.org) | NOT PEER-REVIEWED | Posted: 7 December 2020 doi:10.20944/preprints202012.0170.v1

reduction to ammonia of NOx [110]. This combination allows to achieve an energy requirement of 4.6 MJ·mol^{-1} NH_3, which is more than four times less than the state-of-the-art plasma-enabled ammonia synthesis from N_2 and H_2 with reasonable yields (>1 %). However, this chemistry, although interesting, is not relevant for the scope of this review.

A possibility to improve the performances in NTP is to combine it with a catalyst (plasma-catalysis). The problem is that the mean free path of a gas molecule is about three-four order of magnitude shorter than the typical distance from where they are generated and the catalyst surface in usual plasma-catalysis reactor configurations. Therefore, when N_2* species are formed in the plasma, they collide with many other gas-phase molecules (10^2-10^5 depending on the pressure) and dissipate the energy acquired from the plasma before contacting the catalyst. It should be thus realized the possibility to generate the plasma at the surface or even within the catalyst itself (micro-discharge) [21]. The second issue is that the catalyst should avoid quenching of the generated excited species and react synergistically to control the path of transformation. There are thus still major challenges to develop more effective systems for NH_3 synthesis by plasma-catalysis, but from the perspective of this contribution, the point is to understand which paths have been proposed for ammonia transformation on the surface of the catalyst interacting with N_2* species and thus when the first step of N_2 molecule activation (the usual limiting step at temperatures close to ambient) is overcome by the effect of plasma. Carreon [24] recently summarized the studies on the surface mechanisms proposed in plasma-catalysis for N_2 fixation. Although there are discordances, results can be summarized as follows, depending on the pressure of operation:

- in vacuum plasmas the atomic N species (generated by N_2 dissociation in the plasma) are adsorbed on the catalyst surface and react with atomic H from the gas phase to form NH(s) species and finally ammonia; the rate limiting step is the surface reaction;
- in atmospheric-pressure plasmas, the mechanism is still controversial. One possibility is the dissociative adsorption of excited N_2 as the first reaction step but followed by surface dissociation and then surface hydrogenation by chemisorbed atomic hydrogen species. The other possibility is that atomic nitrogen directly generated in the plasma is chemisorbed and hydrogenated on the surface.

Thus, the mechanisms proposed are close to those occurring in thermal ammonia synthesis catalysis, because the main limit of activation of the N_2 molecule is overcome by the plasma activation. Note that these mechanisms are valid using directly H_2, while become less clear when water is instead present as hydrogen source.

7. Conclusions

The analysis of the molecular mechanisms of solar NH_3 production evidences that there are two groups of mechanisms. The first one occurs either at high temperature (conventional thermal catalysis) and also in plasma-catalysis where the break of the N≡N bond is the first stage, followed by hydrogenation of the nitrogen atoms or NH_x species. The second group of mechanisms, based on the direct hydrogenation of undissociated N_2 molecule, occurs in electrocatalysis, enzymatic catalysis (*Nitrogenase*) and for the most active metal-complexes. We have here not specifically analysed photocatalysis for sake of conciseness, but mechanistic indications are well in line with those discussed for electrocatalysis. These two groups of molecular mechanisms of N_2 fixation have been analysed also in various recent reviews, but the point remarked here is that the consequences of the different initial steps in N_2 fixation are not often then correctly accounted in the proposed mechanisms of reaction.

For this reason, attention has been given here to remark the key features of the proposed mechanism of Nitrogenase, which can be summarized as follows: i) need of a multi-electron and -proton simultaneous transfer, not as sequential steps, ii) formation of bridging metal hydride species, iii) formation of intermediates stabilized by bridging multiple metal atoms, iv) capability of the same sites to be effective both in N_2 fixation and in CO_x reduction to C2+ products. A biomimetic electro (or photo) catalyst should be thus able to have all these features. The only

 doi:10.20944/preprints202012.0170.v1

electrocatalyst we have identified, as far as we know, is based on iron oxide/hydroxide nanoparticles stabilized at defect sites of a nanocarbon support.

In principle also other type of mechanisms could be effective. However, we have also evidenced here, even if not through a fully systematic analysis, that there is currently a very large discordance on the proposed mechanisms for both N_2 fixation and CO_2 multi-carbon (C2+) reduction, despite the limited differences in the performances are not consistent with the large differences in the reaction mechanisms and nature of the active sites. Therefore, at least in terms of the current stage of development it is rather difficult to identify a mechanism which could be the basis for the further development of these (electro)catalysts, while a breakthrough change is requested to go from the current to the needed performances for industrialization of the process.

The biomimetic approach outlined above, and specifically the capability to realize multi-electron/proton simultaneous transfers and activity both in N_2 fixation and CO_2-to-C2+ reduction, we feel could be a relevant source of inspiration to develop the next generation electrocatalysts, which are needed to address the challenging transition to a future sustainable energy and chemistry beyond fossil fuels.

Author Contributions: All authors equally contributed and have read and agreed to the published version of the manuscript.

Funding: This research was partially funded by European Commissions, grant number ERC Synergy SCOPE 810182 and DECADE 862030 and PRIN 2017 project MULTI-e 20179337R7 and CO2 ONLY 2017WR2LRS, which are gratefully acknowledged.

Conflicts of Interest: The authors declare no conflict of interest.

Abbreviations

ATP	Adenosine triphosphate
CNT	Carbon nanotubes
CO_2RR	CO_2 reduction reaction
DFT	Density functional theory
GHG	Greenhouse gas
HB	Haber-Bosch
NHE	Normal hydrogen electrode
NTP	Non-thermal plasma
NRR	Nitrogen reduction reaction
PCET	Proton-coupled electron transfer
PEC	Photoelectrocatalytic
RE	Renewable energy
TON	Turnover number

References

1. Liu, A.; Yang, Y.; Ren, X.; Zhao, Q.; Gao, M.; Guan, W.; M., Fanning; G., L.; Yang, Q.; Liang, X.; et al *ChemSusChem* **2020**, *13*, 3766-3788.
2. MacFarlane, D.R.; Cherepanov, P.V.; Choi, J.; Suryanto, B.H. R.; Hodgetts, R.Y.; Bakker, J.M.; Ferrero Vallana, F.M.; Simonov, A.N. *Joule* **2020**, *4*, 1186-1205.
3. Qing, G.; Ghazfar, R.; Jackowski, S.T.; Habibzadeh, F.; Ashtiani, M.M.; Chen, C.-P.; Smith, M.R.; Hamann, T.W. *Chem. Rev.* **2020**, *120*, 5437-5516.
4. Hochman, G.; Goldman, A.S.; Felder, F.A.; Mayer, J.M.; Miller, A.J. M.; Holland, P.L.; Goldman, L.A.; Manocha, P.; Song, Z.; Aleti, S. *ACS Sustainable Chem. & Eng*. **2020**, *8*, 8938-8948.
5. Lv, X.-W.; Weng, C.-C.; Yuan, Z.-Y. *ChemSusChem* **2020**, *13*, 3061-3078.
6. Xu, H.; Ithisuphalap, K.; Li, Y.; Mukherjee, S.; Lattimer, J.; Soloveichik, G.; Wu, G. *Nano Energy* **2020**, 69, 104469.
7. Smith, C.; Hill, A.K.; Torrente-Murciano, L. *Energy & Env. Science* **2020**, *13*, 331-344.
8. Global Alliance Powerfuels, Powerfuels: Missing link to a successful energy transition, June, 2019.

9. Li, M.; Huang, H.; Low, J.; Gao, C.; Long, R.; Xiong, Y. *Small Methods* **2019**, *3*, 1800388.
10. Wang, Z.; Hu, X.; Liu, Z.; Zou, G.; Wang, G.; Zhang, K. *ACS Catal*. 2019, *9*, 10260-10278.
11. Guo, C.; Ran, J.; Vasileff, A.; Qiao, S.-Z. *Energy & Env. Science* **2018**, *11*, 45-56.
12. Hou, J.; Yang, M.; Zhang, J. *Nanoscale* **2020**, *12*, 6900-6920.
13. Wang, J.; Chen, S.; Li, Z.; Li, G.; Liu, X. *ChemElectroChem* **2020**, *7*, 1067-1079.
14. Qin, Q.; Oschatz, M. *ChemElectroChem* **2020**, *7*, 878-889.
15. Hu, L.; Xing, Z.; Feng, X. *ACS Energy Lett*. **2020**, *5*, 430-436.
16. Zhu, X.; Mou, S.; Peng, Q.; Liu, Q.; Luo, Y.; Chen, G.; Gao, S.; Sun, X. *J. Mater, Chem A* **2020**, *8*, 1545-1556
17. Guo, W.; Zhang, K.; Liang, Z.; Zou, R.; Xu, Q. *Chem. Soc. Rev*. **2019**, *48*, 5658-5716.
18. Wang, Q.; Lei, Y.; Wang, D.; Li, Y. *Energy & Env. Science* **2019**, *12*, 1730-1750.
19. Choi, J.; Suryanto Bryan, H.R.; Wang, D.; Du, H.-L.; Hodgetts, R.Y.; Ferrero Vallana, F.M.; MacFarlane, D.R.; Simonov, A.N.; Choi, J.; Du, H.-L.; et al *Nature Comm*. **2020**, *11*, 5546.
20. Zheng, J.; Lyu, Ya.; Wang, R.; Wang, S.; Zheng, J.; Lyu, Y.; Wang, R.; Wang, S.; Zheng, Ji.; Marco, R. D.; et al *Angew. Chemie Int. Ed*. **2019**, *58*, 18604-18609.
21. Bogaerts, A.; Tu, X.; Whitehead, J. C.; Centi, G.; Lefferts, L.; Guaitella, O.; Azzolina-Jury, F.; Kim, H.-H.; Murphy, A. B.; Schneider, W.F.; et al *J. Phys. D: Appl. Phys.* **2020**, *53*, 443001.
22. Neyts, E.C.; Ostrikov, K.; Sunkara, M. K.; Bogaerts, A. *Chem. Rev.* **2015**, *115*, 13408-13446.
23. Bogaerts, A.; Centi, G. *Frontiers in Energy Res.* **2020**, *8*, 111.
24. Carreon, M.L. *J. Physics D: Appl. Phys*. **2019**, *52*, 483001.
25. Rouwenhorst, K.H.R.; Kim, H.-H.; Lefferts, L. *ACS Sustainable Chem. Eng.* **2019**, *7*, 17515–17522.
26. Cherkasov, N.; Ibhadon, A.O.; Fitzpatrick, P. *Chem. Eng. and Proc.: Process Intensification* **2015**, *90*, 24-33.
27. Hoffman, B.M.; Lukoyanov, D.; Yang, Z.-Y.; Dean, D.R.; Seefeldt, L.C. *Chem. Rev*. **2014**, *114*, 4041-4062.
28. Hu, Y.; Ribbe, M.W. *Angew. Chemie Int. Ed.* **2016**, *55*, 8216-8226.
29. Hu, Y.; Lee, C. C.; Ribbe, M. W. *Science* **2011**, *333*, 753-755.
30. Hu, Y.; Lee, C.C.; Ribbe, M.W. *Dalton Trans*. **2012**, *41*, 1118-1127.
31. Perathoner, S.; Centi, G. *Catal. Today* **2019**, *330*, 157-170.
32. Perathoner, S.; Centi, G. *Catal. Today* **2020**, 342, 4-12.
33. Peng, H.; Tang, M.T.; Liu, X.; Lamoureux, S.P.; Bajdich, M.; Abild-Pedersen, F. *Energy Environ. Sci*. **2020**, Accepted. DOI: 10.1039/D0EE02826F
34. Todorova, T.K.; Schreiber, M.W.; Fontecave, M. *ACS Catal*. **2020**, *10*, 1754-1768.
35. Lei, F.; Yingying, L.; Lei, F.; Chuan, X.; Haotian, W.; Chuan, X.; Fangqi, Y.; Jun, W.; Haotian, W. *Science Adv.* **2020**, *6*, eaay3111.
36. Gao, D.; Sinev, I.; Scholten, F.; Aran-Ais, R.M; Divins, N.J.; Timoshenko, J.; Roldan Cuenya, B.; Sinev, I.; Scholten, F.; Divins, N.J.; et al. *Angew. Chemie Int. Ed*. **2019**, *58*, 17047-17053
37. Chang, X.; Malkani, A.; Yang, X.; Xu, B. *J. Am. Chem. Soc*. **2020**, *142*, 2975−2983.
38. Birdja, Y.Y.; Pérez-Gallent, E.; Figueiredo, M.C.; Göttle, A.J.; Calle-Vallejo, F.; Koper, M.T. M. *Nature Energy* **2019**, *4*, 732–745.
39. Centi, G.; Perathoner, S. *Small* **2020**, submitted.
40. Khare, E.; Yadav, A. *Climate Change and Envir. Sustainability* **2017**, *5*, 122-145.
41. Burgess, B.K.; Lowe, D.J. *Chem. Rev.* **1996**, *96*, 2983-3011.
42. Burgess, B. K. *Chem. Rev*. **1990**, *90*, 1377-1406.
43. Kim, J.; Rees, D. C. *Science* **1992**, *257*, 1677-1682.
44. Spatzal, T.; Aksoyoglu, M.; Zhang, L.; Andrade, S. L. A.; Schleicher, E.; Weber, S.; Rees, D. C.; Einsle, O. *Science* **2011**, *334*, 940.
45. Khadka, N.; Milton, R.D.; Shaw, S.; Lukoyanov, D.; Dean, D.R.; Minteer, S.D.; Raugei, S.; Hoffman, B.M.; Seefeldt, L.C. *JACS* **2017**, *139*, 13518-13524.
46. Lukoyanov, D.; Yang, Z.-Y.; Khadka, N.; Dean, D.R.; Seefeldt, L.C.; Hoffman, B.M. *JACS* **2015**, *137*, 3610-3615
47. Garden, A. L.; Skúlason, E. *J. Phys. Chem. C* **2015**, *119*, 26554-26559.
48. Fuller, J.; Fortunelli, A.; Goddard III, W. A.; An, Q. *Phys. Chem. Chem. Phys*. **2019**, *21*, 11444-11454.
49. Schlögl, R. *Angew. Chemie Int. Ed*. **2003**, *42*, 2004-2008.
50. Schütze, J.; Mahdi, W.; Herzog, B.; Schlögl, R. *Topics Catal*. **1994**, *1*, 195-214.
51. Bazhenova, T.; Shilov, A. *Coord. Chem. Rev*. **1995**, *144*, 69–145.
52. Ghosh, A. C.; Duboc, C.; Gennari, M. *Coord. Chem. Rev*. **2021**, *428*, 213606.

53. Rebelein, J.G.; Hu,Y.; Ribbe, M.W. *Angew. Chemie Int. Ed*. **2014**, *53*, 11543-11546.
54. Seefeldt, L.C.; Yang, Z.-Y.; Lukoyanov, D.A.; Harris, D.F.; Dean, D.R.; Raugei, S.; Hoffman, B.M. *Chem. Rev*. **2020**, *120*, 5082-5106.
55. Rettberg, L.A.; Stiebritz, M.T.; Kang, W.; Lee, C.C.; Ribbe, M.W.; Hu, Y. *Chem, - A Europ. J.* **2019**, *25*, 13078-13082.
56. Lee, H.-I.; Sorlie, M.; Christiansen, J.; Yang, T.-C.; Shao, J.; Dean, D.R.; Hales, B. J.; Hoffman, B.M. *JACS* **2005**, *127*, 15880-15890.
57. Jia, H.-P.; Quadrelli, E.A. *Chem. Soc. Rev*. **2014**, *43*, 547–564.
58. Lukoyanov, D.; Khadka, N.; Yang, Z.-Y.; Dean, D.R.; Seefeldt, L.C.; Hoffman, B.M. *JACS* **2016**, *138*, 10674–10683.
59. Seefeldt, L.C.; Hoffman, B.M.; Dean, D.R. Annu. Rev. Biochem 2009, 78. 701-722.
60. Bjornsson, R.; Lima, F.A.; Spatzal, T.; Weyhermueller, T.; Glatzel, P.; Bill, E.; Einsle, O.; Neese, F.; DeBeer, S. *Chem. Sci*. **2014**, *5*, 3096–3103.
61. Nagelski, A.L.; Fataftah, M.S.; Bollmeyer, M.M.; McWilliams, S.F.; MacMillan, S.N.; Mercado, B.Q.; Lancaster, K.M.; Holland, P.L. Chem. Sci. 2020, Ahead of Print. DOI: 10.1039/D0SC03447A.
62. Chalkley, M.J.; Drover, M.W.; Peters, J.C. *Chem. Rev*. **2020**, *120*, 5582–5636.
63. Singh, D.; Buratto, W.R.; Torres, J.F.; Murray, L.J. *Chem. Rev*. **2020**, *120*, 5517-5581.
64. Tanifuji, K.; Ohki, Y. *Chem. Rev*. **2020**, *120*, 5194–5251.
65. Yandulov, D. V.; Schrock, R. R. *Science* **2003**, *301*, 76−78.
66. Anderson, J. S.; Moret, M. E.; Peters, J. C. *JACS* **2013**, *135*, 534−537.
67. Centi, G.; Perathoner, S.; Winè, G.; Gangeri, M. *Green Chem*. **2007**, *9*, 671-678.
68. Gangeri, M.; Perathoner, S.; Caudo, S.; Centi, G.; Amadou, J.; Begin, D.; Pham-Huu, C.; Ledoux, M. J.; Tessonnier, J.-P.; Su, D. S.; Schlögl, R. *Catal. Today* **2009**, *143*, 57-63.
69. Huang, Y.; Handoko, A. D.; Hirunsit, P.; Yeo, B. S. *ACS Catal.* **2017**, *7*, 1749-1756.
70. Schouten, K. J. P.; Qin, Z.; Gallent, E. P.; Koper, M. T. M. *JACS* **2012**, *134*, 9864-9867.
71. Kortlever, R.; Shen, J.; Schouten, K.J.P.; Calle-Vallejo, F.; Koper, M.T.M., *J. Phys. Chem. Lett*. **2015**, *6*, 20, 4073–4082.
72. Montoya, J. H.; Shi, C.; Chan, K.; Nørskov, J. K. *J. Phys. Chem. Lett*. **2015**, *6*, 2032-2037.
73. Goodpaster, J.D.; Bell, A. T.; Head-Gordon, M. *J. Phys. Chem. Lett*. **2016**, *7*, 1471–1477.
74. Chang, X.; Malkani, A.; Yang, X.; Xu, B. *JACS* **2020**, *142*, 2975–2983.
75. Chan, Y.-T.; Huang, I-S.; Tsai, M.-K. *Phys. Chem. Chem. Phys*., **2019**, *21*, 22704-22710.
76. Chen, S.; Perathoner, S.; Ampelli, C.; Mebrahtu, C.; Su, D.S.; Centi, G. *Angew. Chemie Int. Ed*. **2017**, *56*, 2699-2703.
77. Chen, S.; Perathoner, S.; Ampelli, C.; Mebrahtu, C.; Su, D.S.; Centi, G. *ACS Sustainable Chem. & Eng*. **2017**, 5, 7393-7400.
78. Chen, S.; Perathoner, S.; Ampelli, C.; Wei, H.; Abate, S.; Zhang, B.; Centi, G. *ChemElectroChem* **2020**, *7*, 3028-3037.
79. Genovese, C.; Schuster, M. E.; Gibson, E. K.; Gianolio, D.; Posligua, V.; Grau-Crespo, R.; Cibin, G.; Wells, P. P.; Garai, D.; Solokha, V.; Calderon, S. K.; Velasco-Velez, J. J.; Ampelli, C.; Perathoner, S.; Held, G.; Centi G.; Arrigo, R. *Nature Comm*. **2018**, *9*, 935.
80. Chen, S.; Perathoner, S.; Ampelli, C.; Wei, H.; Abate, S.; Zhang, B.; Centi, G. *J. Energy Chem*. **2020**, *49*, 22-32.
81. Wang, T.; Xia, L.; Yang, J.-J.; Wang, H.; Fang, W.-H.; Chen, H.; Tang, D.; Asiri, A. M.; Luo, Y.; Cui, G.; Sun, X. *Chem. Commun*. **2019**, *55*, 7502-7505.
82. Yu, X.; Han, P.; Wei, Z.; Huang, L.; Gu, Z.; Peng, S.; Ma, J.; Zheng, G. *Joule* **2018**, *2*, 1610-1622.
83. Yuan, L.-P.; Wu, Z.-Y.; Jiang, W.-J.; Tang, T.; Niu, S.; Hu, J.-S. *Nano Res.* **2020**, *13*, 1376-1382
84. Liu, Y.; Su, Y.; Quan, X.; Fan, X.; Chen, S.; Yu, H.; Zhao, H.; Zhang, Y.; Zhao, J. *ACS Catal*. **2018**, 8, 1186-1191.
85. Liu, Z.; Zhang, M.; Wang, H.; Cang, D.; Ji, X.; Liu, B.; Yang, W.; Li, D.; Liu, J. ACS Sustainable Chem. Eng. **2020**, *8*, 5278-5286.
86. Yin, H.; Gan, L.-Y.; Wang, P. *J. Mater. Chem. A* **2020**, *8*, 3910-3917.
87. Cao, Y.; Deng, S.; Fang, Q.; Sun, X.; Zhao, C.X.; Zheng, J.; Gao, Y.; Zhuo, H.; Li, Y.; Yao, Z. *Nanotechn*. **2019**, *30*, 335403.
88. Mukherjee, S.; Yang, X.; Shan, W.; Samarakoon, W.; Karakalos, S.; Cullen, D. A.; More, K.; Wang, M.; Feng, Z.; Wang, G.; Wu, G. *Small Methods* **2020**, *4*, 1900821.

89. Wang, S.; Shi, L.; Bai, X.; Li, Q.; Ling, C.; Wang, J. *ACS Cent. Sci*. **2020**, *6*, 1762-1771.
90. Xu, F.; Zhang, L.; Ding, X.; Cong, M.; Jin, Y.; Chen, L.; Gao, Y. *Chem. Commun*. **2019**, *55*, 14111-14114.
91. Lai, F.; Feng, J.; Ye, X.; Zong, W.; He, G.; Yang, C.; Wang, W.; Miao, Y.-E.; Pan, B.; Yan, W.; Liu, T.; Parkin, I. P. *J. Mater. Chem. A* **2020**, *8*, 1652-1659.
92. Zhang, S.; Li, W.; Liu, Y.; Wang, J.; Wang, G.; Zhang, Y.; Han, M.; Zhang, H. *Inorg. Chem. Frontiers* **2019**, *6*, 2832-2836.
93. Eilert, A.; Roberts, F. S.; Friebel, D.; Nilsson, A. *J. Phys. Chem. Lett*. **2016**, *7*, 1466–1470.
94. Munir, S.; Varzeghani, A. R.; Kaya, S. *Sustainable Energy Fuels* **2018**, *2*, 2532–2541.
95. Li, Y.; Kim, D.; Louisia, S.; Xie, C.; Kong, Q.; Yu, S.; Lin, T.; Aloni, S.; Fakra, S.C.; Yang, P. *PNAS* **2020**, *117*, 9194-9201.
96. Zhuang, T.-T.; Pang, Y.; Liang, Z.-Q.; Wang, Z.; Li, Y.; Tan, C.-S.; Li, J.; Dinh, C. T.; De Luna, P.; Hsieh, P.-L. et al *Nature Catal*. **2018**, *1*, 946-951.
97. Zhang, B.-B.; Wang, Y.-H.; Xu, S.-M.; Chen, K.; Yang, Y.-G.; Kong, Q.-H. *RSC Adv*. **2020**, *10*, 19192-19198.
98. Sen, S.; Liu, D.; Palmore, G. T. R. *ACS Catal*. **2014**, *4*, 3091–3095.
99. Lum, Y.; Yue B.; Lobaccaro, P.; Bell, A. T.; Ager, J. W. *J. Phys. Chem. C* **2017**, *121*, 14191–14203.
100. Genovese, C.; Ampelli, C.; Perathoner, S.; Centi, G. *Green Chem*. **2017**, *19*, 2406-2415.
101. Marepally, B. C.; Ampelli, C.; Genovese, C.; Tavella, F.; Quadrelli, E. A.; Perathoner, S.; Centi, G. *J. CO_2 Utiliz*. **2020**, *35*, 195-204.
102. Han, H.; Noh, Y.; Kim, Y.; Park, S.; Yoon, W.; Jang, D.; Choi, S. M.; Kim, W. B. *Green Chem*. **2020**, *22*, 71.84.
103. Eren, B.; Zherebetskyy, D.; Patera, L.L.; Wu, C.H.; Bluhm, H.; Africh, C.; Wang, L.W.; Somorjai, G.A.; Salmeron, M. *Science* **2016**, *351*, 475–478.
104. Kuhl, K.P.; Cave, E.R.; Abram, D.N.; Jaramillo, T.F. *Energy & Envir. Science* **2012**, *5*, 7050-7059.
105. Genovese, C.; Ampelli, C.; Perathoner, S.; Centi, G. *J. Catal.* **2013**, *308*, 237-249.
106. Ampelli, C.; Centi, G.; Passalacqua, R.; Perathoner, S. *Energy & Envir. Science* **2010**, *3*, 292-301.
107. Ampelli, C.; Genovese, C.; Marepally, B.C.; Papanikolaou, G.; Perathoner, S.; Centi, G. *Faraday Discuss*. **2015**, *183*, 125-145.
108. Marepally, B. C.; Ampelli, C.; Genovese, C.; Saboo, T.; Perathoner, S.; Wisser, F. M.; Veyre, L.; Canivet, J.; Quadrelli, E. A.; Centi, G. *ChemSusChem* **2017**, *10*, 4442-4446.
109. Shi, R.; Zhang, X.; Waterhouse, G.I.N.; Zhao, Y.; Zhang, T. *Adv. Energy Mater*. **2020**, *10*, 2000659.
110. Hollevoet, L.; Jardali, F.; Gorbanev, Y.; Creel, J.; Bogaerts, A.; Martens, J.A. *Angew. Chemie Int. Ed*., **2020**, Early view. DOI: 10.1002/anie.202011676